Version of Record: https://www.sciencedirect.com/science/article/pii/S0960852416310999
Manuscript_0f2437a48bb04d5760d3b7b024d9946a

Light intensity impacts the production of biofuel intermediates in *Heterosigma akashiwo* growing on simulated flue gas containing carbon dioxide and nitric oxide

Colleen M. Bianco[a], Jennifer J. Stewart[a]*, Katherine R. Miller[c], Catherine Fitzgerald[c], Kathryn J. Coyne[a]

[a] University of Delaware, School of Marine Science and Policy, Lewes, DE 19958, USA
[c] Department of Chemistry, Salisbury University, Salisbury, MD 21801, USA

* Corresponding Author:
700 Pilottown Rd, Lewes, DE 19958 USA
302-645-4371
jen@udel.edu

© 2016 published by Elsevier. This manuscript is made available under the Elsevier user license
https://www.elsevier.com/open-access/userlicense/1.0/

Abstract

As a potential biofuel feedstock, the marine microalga, *Heterosigma akashiwo*, accumulates significant lipids, is capable of long-term growth in outdoor photobioreactors, and is an excellent candidate for the bioremediation of industrial emissions. Here, we evaluated resource partitioning in *H. akashiwo* growing on a CO_2 and NO gas mixture under three light intensities: 160, 560, or 1200 µmol quanta m^{-2} s^{-1}. Light levels had no effect on growth; however, cultures in high light accumulated 2.3-fold more carbohydrates and 17% fewer lipids. Light levels did not affect the percentage of saturated fatty acids, but mono-unsaturates increased by 6% and poly-unsaturates decreased by 12% in high light. The fatty acid profiles reported here suggest that *H. akashiwo* is a good candidate for the production of neutral lipids for biodiesel and also omega-3 fatty acids, and that the quality of biodiesel acquired from feedstocks grown under fluctuating light conditions would be relatively stable.

Keywords: *Heterosigma*, biofuel, irradiance, carbohydrate, bioremediation

1. Introduction

Microalgae are receiving significant attention as a viable feedstock for the production of sustainable biofuels and bioproducts, but algae-derived commodity products are not yet cost competitive with their petroleum-derived counterparts (Davis et al., 2014). Since biomass production accounts for 73% of the final selling price for algal biofuels (Davis et al., 2012), reducing costs associated with farming algae will be essential for overcoming the barriers to economic production of algal bioproducts.

CO_2 supplementation is a costly requirement for commercial biomass production due to carbon limitation at atmospheric CO_2 levels (Benemann 2013), so developing

25 innovative CO_2 utilization strategies could decrease operating costs significantly.
26 Utilizing waste CO_2 from industrial emissions (i.e. flue gases) would have the dual
27 advantage of simultaneously decreasing biomass production costs while also mitigating
28 the effects of harmful greenhouse gas emissions. Fossil fuel-burning power plants are
29 responsible for over 30% of total greenhouse gas emissions in the United States, and
30 Environmental Protection Agency's Clean Power Plan supports the use of algae-based
31 carbon capture and reuse technologies for power plants to meet new emissions standards
32 (EPA, 2015).

33 In addition to CO_2, flue gas also contains cytotoxic nitrogen oxides (NOx, >90%
34 as nitric oxide), and the reaction products of NOx emissions, ozone (O_3) and nitrous
35 oxide (N_2O), are also potent greenhouse gases (EPA 2014). Previously, we have shown
36 that the marine microalga, *Heterosigma akashiwo* (Raphidophyceae), is an excellent
37 candidate for the bioremediation of industrial emissions, since this alga has the ability to
38 metabolize gaseous nitric oxide (NO) as a nitrogen source (Stewart and Coyne, 2011),
39 and that cultivation on a model flue gas had a positive effect on the growth and
40 productivity of biofuel intermediates in this organism (Stewart et al., 2015). Elsewhere,
41 *H. akashiwo* has been identified as a promising biofuel feedstock (Fuentes-Grünewald et
42 al., 2009) that accumulates significant lipid reserves (Fuentes-Grünewald et al., 2012) and
43 is capable of stable long-term growth in outdoor photobioreactors (Fuentes-Grunewald et
44 al., 2013). Harnessing both CO_2 and NOx emissions from flue gas as carbon and nitrogen
45 nutrient sources for the growth of microalgae could theoretically reduce operating costs
46 for biomass production by 50% (Douskova et al., 2009; Nagarajan et al., 2013), making
47 *H. akashiwo* an attractive candidate for large scale cultivation.

48 *H. akashiwo* is a robust organism that is found in temperate and subtropical
49 regions worldwide (Tobin et al., 2013). Under natural conditions, this alga preferentially
50 migrates to the water surface at mid-day (peak light), and naturally blooms in surface
51 waters where light can exceed 2000 µmol quanta m^{-2} s^{-1} (Handy et al., 2005). *H. akashiwo*
52 can grow under a wide range of salinities (5-30 psu), temperatures (4-30 °C), and nutrient
53 regimes (Zhang et al., 2006). The ability of *H. akashiwo* to maintain growth under
54 suboptimal conditions may be due in part to its high photosynthetic efficiency and its
55 ability to rapidly exploit high-light and stratified-light environments (Hennige et al.,
56 2013).

57 Light intensity has been shown to alter fatty acid composition (e.g. Solovchenko
58 and Khozin-Goldberg, 2013) and starch synthesis (e.g. Li et al., 2010) in microalgae.
59 Under saturating irradiances, many microalgae alter their lipid biosynthetic pathways to
60 accumulate saturated and mono-unsaturated fatty acids (e.g. Hu et al., 2008). Saturated
61 fatty acids are the precursors to quality biodiesel, but supplying maximum light intensity
62 without inducing photodamage presents a difficult challenge. *H. akashiwo* resists
63 photodamage by rapidly acclimating to high-light intensities by utilizing cellular
64 mechanisms to induce photoprotection, such as nonphotochemical quenching and
65 reduced PSII reaction center connectivity (Hennige et al., 2013). These photo-protective
66 mechanisms make *H. akashiwo* a good candidate for the optimization of lipid quality and
67 quantity by light manipulation.

68 Here, we examined the effect of light intensity on resource partitioning and the
69 production of biofuel intermediates in *H. akashiwo* previously acclimated to growth on a
70 simulated flue gas. High light intensities did not inhibit the growth of *H. akashiwo*, and

71 did not significantly alter the calculated biodiesel quality of *H. akashiwo*-derived
72 FAMEs. After theoretical extraction of high value eicosapentaenoic acid (EPA;
73 C20:5n3), the calculated values for cetane number (CN) met the American Society for
74 Testing Materials (ASTM) minimums for 100% biodiesel stocks.

75 **2. Materials and Methods**

76 *2.1. Culture Conditions*

77 Stocks of *Heterosigma akashiwo* CCMP 2393 (NCMA; Boothbay Harbor, ME) were
78 maintained in 20 ppt salinity f/2 (-Si) medium (Guillard, 1975) buffered at pH 7.4 with 20
79 mM HEPES (Sigma-Aldrich, St. Louis, MO, USA) at 25 °C on a 12:12 hour light: dark
80 cycle with an irradiance of 100 μmol quanta m^{-2} s^{-1}, and bubbled with a model flue gas
81 (12% CO_2, 150 ppm NO, balanced in N_2; Praxair Technologies, Danbury, CT, USA) for
82 3 months before the experiment.

83

84 *2.2. Experimental Design*

85 Replicate cultures (500 mL; N=4) were acclimated to increasing PAR levels: 160,
86 560, or 1200 μmol quanta m^{-2} s^{-1} (herein defined as low-, medium-, and high-light,
87 respectively) on a 12:12 hour light: dark cycle. After six weeks of growth at the
88 respective light intensity, replicate cultures were maintained semi-continuously in
89 exponential growth. Cultures were diluted to 150,000 cells/mL every other day. Cell
90 counts, *in vivo* chlorophyll a (chl *a*), extracted chl *a*, and quantum efficiency of
91 photosystem II (F_v/F_m) were measured every other day before cultures were diluted to
92 monitor the cultures for steady state growth. Steady state growth was reached when cell
93 counts and extracted chl *a* did not vary between dilution days by 5%. Samples were

94 collected for analysis of total lipid content, fatty acid composition, carbohydrate and
95 protein content, and particulate carbon and nitrogen after 10 days of steady state growth.
96 For cell counts, cells were fixed in a 2% gluteraldehyde solution then counted on a
97 hemeocytometer. Growth rates were calculated as:

98 μ=Ln(N_2/N_1)]/(t_2-t_1),

99 where N is the cell number (cells/mL) and t is the time in days.

100 *In vivo* chl *a* fluorescence was measured using an AquaFluor handheld
101 fluorometer (Turner Designs, Sunnyvale, CA, USA). Chl *a* was extracted overnight at -20
102 °C in 90% acetone and measured using a 10AU field fluorometer (Turner Designs,
103 Sunnyvale, CA, USA).

104 *2.3. Fast Repetition Rate Fluorometry*

105 Maximum quantum yield of PSII fluorescence (F_v/F_m) was measured from a 1 ml
106 sub-sample of culture using a Fast Repetition Rate fluorometer (FRRf, FastOcean FRR
107 plus FastAct Laboratory System, Chelsea Technologies Group Ltd, United Kingdom).
108 Samples were low-light acclimated for 20 min then dark acclimated for 2 min prior to
109 measuring F_v/F_m as previously optimized for photosynthetic measurements of *H.*
110 *akashiwo* (Hennige et al., 2013). For determination of electron transport rates, a bank of
111 white LEDs within the FastAct was set to deliver an irradiance of 150, 500, or 1200 µmol
112 quanta m^{-2} s^{-1} for a 5 min interval prior to the measurement. The electron transport rate
113 (ETR) through photosystem II (PSII) in µmol e^- m^{-2} s^{-1} was calculated as:

114 $$ETR_{(PSII)} = Fq'/Fm' \; x \; E$$

115 where *Fm'* is the maximal fluorescence yield in the light acclimated state, *Fq'* is the
116 difference between *Fm'* and the steady state fluorescence measured under actinic light
117 (i.e. *F*), and *E* is the incident photosynthetically active radiance (PAR).

118 *2.4. Transesterification and Analysis of Fatty Acids*

119 Fatty acid methyl esters (FAMEs) were prepared by acid catalyzed direct
120 transesterification and analyzed by gas chromatography as previously described by
121 Stewart et al. (2015).

122 *2.5. Total Lipid, Carbohydrate, and Protein Quantification*

123 Total lipids, carbohydrates, and proteins were quantified by colorimetric methods
124 as previously described by Stewart et al. (2015).

125 *2.6. Particulate Carbon and Particulate Nitrogen*

126 Particulate carbon and particulate nitrogen were quantified using a particulate
127 autoanalyzer (Costech Elemental Analyzer, Costech Analytical Technologies) and
128 standard techniques (Hutchins, 2002). Briefly, the algal cultures were filtered onto
129 precombusted GF/F Whatman glass-fiber filters, stored at -80 °C then dried in an 80 °C
130 oven prior to analysis. Phenylalanine and ethylenediaminetetraacetic acid were used as
131 standards.

132 *2.7. Estimation of Biodiesel Parameters*

133 The saponification number (SN), iodine number (IN), and cetane number (CN)
134 were estimated using empirical formulas from Lei et al. (2012) as previously described
135 by Stewart et al. (2015).

136 *2.8. Statistical Analysis*

137 The experiment was performed in replicate (N=4) for each light level. Data
138 represents means ± standard deviations. Statistical analysis was performed using JMP
139 Pro v12 software (SAS, Cary, NC, USA). Prior to comparison of means, data were
140 assessed for normality and equality of variance. Raw data that did not meet assumptions
141 of equal variance (by Levene's test) and/or normality (by the Shapiro-Wilk W test) were
142 transformed prior to statistical analysis. A p-value < 0.05 was used as the standard for
143 statistical significance. One-Way Analysis of Variance (ANOVA) was used to determine
144 statistical significance among the light levels followed by Tukey's HSD *post hoc*
145 analysis. For non-parametric analyses, the Kruskal-Wallis Rank Sums test was applied
146 followed by Steel-Dwass *post hoc* analysis.

147 **3. Results and Discussion**

148 *3.1. Growth Rates and Photosynthesis*

149 In this study, *H. akashiwo* was cultured with a model flue gas under light
150 intensities ranging from 160 to 1200 μmol quanta m^{-2} s^{-1}. Previous studies on algae have
151 shown that irradiance above the level of light saturation will cause a decrease in growth
152 rate due to photoinhibition (Rawat et al., 2013). In contrast, there were no significant
153 differences in growth rates or biomass among the light intensities used in this study
154 (Table 1), showing that *H. akashiwo* (CCMP 2393) is not photoinhibited at intensities
155 equal to or below 1200 μmol quanta m^{-2} s^{-1}. For each treatment, the maximum electron
156 transport rate through photosystem II ($ETR_{(PSII)}$) increased with exposure to increasing
157 PAR settings in *H. akashiwo* (Fig. 1), similar to the response of another closely related
158 raphidophyte, *Chattonella subsalsa* (Warner and Madden, 2007). Notably, $ETR_{(PSII)}$

159 values for low-light acclimated cultures were significantly higher than or equal to those
160 for cultures acclimated at medium- and high-light levels when exposed to any of the three
161 PAR settings ($P < 0.02$). For a given PAR intensity (150, 500, or 1200 μmoles quanta m^{-2}
162 s^{-1}), there were no significant differences between $ETR_{(PSII)}$ for the medium- and high-
163 light acclimated cultures. Within treatments, $ETR_{(PSII)}$ peaked when exposed to 500
164 μmoles quanta m^{-2} s^{-1} for both the low-light and high-light acclimated cultures ($P < 0.01$),
165 while $ETR_{(PSII)}$ was highest when exposed to 1200 μmoles quanta m^{-2} s^{-1} for the medium
166 light acclimated culture ($P < 0.001$). These results corroborate previous work, which
167 showed that this strain of *H. akashiwo* rapidly acclimates to shifts in light intensity by
168 utilizing novel photoprotection strategies that enable the alga to exploit high-light
169 regimes in order to rapidly increase growth rates (Hennige et al., 2013). Since light
170 saturation was not observed for the light levels used in the current study, further studies
171 on the photobiology of *H. akashiwo* at very high light intensities (>1200 μmoles quanta
172 m^{-2} s^{-1}) would be valuable.
173 Stable growth rates and rapid ETR responses across light levels are key attributes
174 for successful large-scale cultivation of microalgae in an outdoor commercial setting,
175 where light intensity fluctuates with the weather. Open raceway ponds are commonly
176 used during the mass cultivation of microalgae for biodiesel; however, light limitation
177 due to shading in dense cultures contributes to the low productivities typically seen in
178 open ponds (Rawat et al., 2013). Presumably, the ability of *H. akashiwo* to rapidly exploit
179 fluctuating light intensities contributes to the formation of high-density algal blooms in
180 the natural environment (Hennige et al., 2013). Our study indicates that *H. akashiwo*
181 could be equally productive at the pond surface where irradiance is very high, as well as

182 below the surface where irradiance is attenuated, and would also be able to exploit the
183 rapidly changing light levels that are characteristic of turbulent mixing conditions.

184 *3.2. Resource Partitioning*

185 The biochemical composition (protein, lipid, and carbohydrate) of *H. akashiwo*
186 varied with light intensity (Fig. 2). Carbohydrate content (pg/cell) was the predominant
187 biochemical constituent for all light treatments, which is not surprising as β-1, 3-glucans
188 are the main storage products of photosynthesis in *H. akashiwo* (Takahashi et al., 2013).
189 Compared to *H. akashiwo* grown in low light, the cultures grown in high light
190 accumulated 2.3-fold more carbohydrates ($P < 0.05$) and 17% fewer lipids ($P < 0.01$; Fig.
191 2). The decrease in lipids observed here is in contrast to the general trend for microalgae,
192 where lipid content increases with light intensity. Our data reinforces the hypothesis that
193 carbohydrates are the preferred energy storage molecules in *H. akashiwo* when neither
194 light nor CO_2 are limiting. Carbohydrate accumulation is a more efficient energy storage
195 strategy because less ATP and NAD(P)H per carbon are required for carbohydrate
196 synthesis versus TAG synthesis (reviewed in Subramanian et al., 2013). Although TAGs
197 have a higher energy density than storage carbohydrates, it is not enough to compensate
198 for the energy invested in TAG synthesis (Subramanian et al., 2013).

199 The particulate carbon to particulate nitrogen ratio (C/N) in the high-light
200 treatment was significantly higher than in the low-light treatment (6.33 ± 0.2 and 5.48 ±
201 0.06, respectively; $P < 0.01$; Table 1). Neither carbon nor nitrogen content (pg/cell)
202 varied significantly between low- and high-light treatments, but *H. akashiwo* grown in
203 low-light produced 2.8-fold more chl *a* ($P < 0.03$; Fig. 2) and the accumulation of
204 carbohydrates in *H. akashiwo* grown under high light coincided with a trend in

205 decreasing protein content. These results suggest that *H. akashiwo* may be partitioning
206 nitrogen into nitrogen-containing carbohydrates rather than protein at higher irradiances
207 (e.g. Chizhov et al., 1998). Additionally, Hennige et al. (2013) noted that one of *H.*
208 *akashiwo's* strategies for photoprotection in response to high-light might occur through a
209 shift in metabolic demands, where the cell maintains a high carbohydrate to protein ratio
210 and high respiration rate to compensate for low non-photochemical quenching (NPQ).
211 Therefore, the extreme accumulation of carbohydrates in response to increasing light seen
212 here may be a contributing factor to the success of the alga at 1200 µmoles quanta m^{-2} s^{-1}
213 and the apparent lack of light saturation at this level.

214 *3.4. Fatty Acid Analysis and Biodiesel Quality*

215 Fatty acid profiles were determined to assess the effects of light intensity on the
216 biodiesel potential of *H. akashiwo* (Fig. 3). The major fatty acids (>5% total FAMEs) in
217 all three treatments were myristic (C14:0), palmitic (C16:0), palmitoleic (C16:1),
218 linolenic (C18:3), stearidonic (C18:4), and eicosapentaenoic (C20:5n3, EPA). Light
219 levels did not affect the percent of SAFAs, but MUFAs increased by 6% ($P < 0.03$) and
220 PUFAs decreased by 12% ($P < 0.05$) from low-light to high-light (Table 2). At the
221 individual fatty acid level, a significant increase in the synthesis of C14:0 (5.1%), C16:0
222 (5.5%) and C16:1 (4.3%) and a concurrent significant decrease in C18:4 (7.0%) and
223 C20:5n3 (3.9%) was observed with increasing light levels ($P < 0.05$). These results agree
224 with other studies that have shown that PUFAs are reduced under high-light conditions,
225 since they are the major structural lipids of thylakoid membranes, while SAFAs and
226 MUFAs are stored as triacylglycerol in cytosolic lipid bodies (Richmond and Hu, 2013).
227 Additionally, the significant increase in C14:0 with increasing light can be explained by

228 its requirement for the synthesis of C16:0, since C14:0 is linked to the fatty acid synthase
229 enzyme prior to the two carbon elongation cycle that produces C16:0. Here, it appears
230 that the significant changes in individual fatty acid content are driven by the
231 photosynthetic requirements of cultures growing under different light regimes.

232 In microalgae, only fatty acids that form triacylglycerides are easily converted
233 into biodiesel, and the fatty acid composition of these neutral lipids determines biodiesel
234 quality. Therefore, FAME profiles and empirical formulas may be used to estimate a
235 cetane number (CN), which is the primary indicator of diesel quality that measures the
236 ignition delay when diesel is injected into a combustion chamber (Lei et al., 2012). A
237 higher CN indicates a shorter ignition time. The American Society for Testing Materials'
238 minimum CN requirement is 40 for blended (6% to 20%) biodiesel and 47 for 100%
239 biodiesel (ASTM, 2014). In the present study, light levels did not significantly affect CN,
240 and the CNs for FAMEs derived from medium- and high-light cultures were appropriate
241 for blended biodiesel stocks (Table 3). Since CN increases with increasing fatty acid
242 chain length and decreases with increasing degree of unsaturation, EPA (C20:5n3), which
243 was the third most abundant fatty acid in all three treatments, decreased the estimated CN
244 for *H. akashiwo*-derived FAMEs. EPA is an economically valuable omega-3 fatty acid,
245 and it is commercially feasible to recover about 70% of the EPA fraction (Molina Grima
246 et al., 2003). Based on this assumption, removal of EPA would increase the CN value to
247 between 48-53 for all treatments, which is above the US standard for 100% biodiesel
248 (Table 3). These estimated values are on par with the CN of soybean oil (51), currently
249 used for biodiesel in the United States (Hu et al. 2008).

250 **4. Conclusions**

251 Overall, the fatty acid profiles reported in this study suggest that *H. akashiwo* is a
252 good candidate for the production of biodiesel and EPA as a valuable co-product.
253 Additionally, the quality of biodiesel acquired from *H. akashiwo* grown under fluctuating
254 light conditions would be relatively stable. Cultures were not photoinhibited, nor did they
255 reach light saturation at 1200 µmoles quanta m^{-2} s^{-1}, indicating that *H. akashiwo* would
256 perform well in outdoor conditions. Our results also reinforce that carbohydrates are the
257 preferred energy storage molecules in *H. akashiwo*, which may be a good source of
258 fermentable carbon for bioethanol production.

259

260 **Acknowledgements**

261 This work was supported by the United States Department of Agriculture (USDA-NIFA-
262 2011-67012-31175 to J.J.S.), the National Oceanic and Atmospheric Administration
263 through Delaware Sea Grant (Award #NA10OAR4170084-12 to K.J.C. and J.J.S. and
264 Award #NA14OAR4170087 to J.J.S. and K.J.C.), and the National Science Foundation
265 (Award #1314003 to J.J.S.). The authors would like to thank Kenneth Hoadley
266 (University of Delaware) for engineering assistance and Mark Warner (University of
267 Delaware) for technical support. A portion of this work resulted from the Masters Thesis
268 of C. Bianco at the University of Delaware.

269

270 **References**

271 1. American Society for Testing Materials International, 2014. Standard specification for
272 biodiesel fuel blend stock (B100) for middle distillate fuels. Standard Designation
273 D6751-14.

274 2. Benemann, J., 2013. Microalgae for biofuels and animal feeds. Energies 6, 5869–5886.

275 3. Chizhov, A.O., Dell, A., Morris, H.R., Reason, A.J., Haslam, S.M., Mcdowell, R.A.,
276 Chizhov, O.S., Usov, A.I., 1998. Structural analysis of laminarans by MALDI and
277 FAB mass spectrometry. Carbohydr. Res. 310, 203–210.

278 4. Davis, R.E., Fishman, D.B., Frank, E.D., Johnson, M.C., Jones, S.B., Kinchin, C.M.,
279 Skaggs, R.L., Venteris, E.R., Wigmosta, M.S., 2014. Integrated evaluation of
280 cost, emissions, and resource potential for algal biofuels at the national scale.
281 Environ. Sci. Technol. 48, 6035–6042.

282 5. Davis, R., Fishman, D., Frank, E.D., Wigmosta, M.S., Aden, A., Coleman, A.M.,
283 Pienkos, P.T., Skaggs, R.J., Venteris, E.R., Wang, M.Q., June 2012. Renewable
284 diesel from algal lipids: An integrated baseline for cost, emissions, and resource
285 potential from a harmonized model. ANL/ESD/12-4; NREL/TP-5100-55431;
286 PNNL-21437. Argonne, IL: Argonne National Laboratory; Golden, CO: National
287 Renewable Energy Laboratory; Richland, WA: Pacific Northwest National
288 Laboratory.

289 6. Douskova, I., Doucha, J., Livansky, K., Machat, J., Novak, P., Umysova, D.,
290 Zachleder, V., Vitova, M., 2009. Simultaneous flue gas bioremediation and

291 reduction of microalgal biomass production costs. Appl. Microbiol. Biotechnol.
292 82, 179–185.
293 7. Environmental Protection Agency, 2014. Air emission sources: Nitrogen Oxides
294 http://www.epa.gov/air/emissions/nox.htm Retrieved 9/16/2010.
295 8. Environmental Protection Agency, 2015. 40 CFR part 60 Carbon pollution emission
296 guidelines for existing stationary sources: Electric utility generating units; final
297 rule. Federal Register 80(205), 64884.
298 9. Fuentes-Grunewald, C., Garces, E., Alacid, E., Rossi, S., Camp, J., 2013. Biomass and
299 lipid production of dinoflagellates and raphidophytes in indoor and outdoor
300 photobioreactors. Mar. Biotechnol. 15, 37–47.
301 10. Fuentes-Grünewald, C., Garcés, E., Alacid, E., Sampedro, N., Rossi, S., Camp, J.,
302 2012. Improvement of lipid production in the marine strains *Alexandrium*
303 *minutum* and *Heterosigma akashiwo* by utilizing abiotic parameters. J. Ind.
304 Microbiol. Biot. 39, 207–216.
305 11. Fuentes-Grünewald, C., Garcés, E., Rossi, S., Camp, J., 2009. Use of the
306 dinoflagellate *Karlodinium veneficum* as a sustainable source of biodiesel
307 production. J. Ind. Microbiol. Biot. 36, 1215–1224.
308 12. Guillard, R.R.L., 1975. Culture of phytoplankton for feeding marine invertebrates. In:
309 *Culture of Marine Invertebrate Animals* (Smith, W.L., Chanley, M.H., eds), pp
310 26–60. New York: Plenum Press.
311 13. Handy, S.M., Coyne, K.J., Portune, K.J., Demir, E., Doblin, M.A., Hare, C.E., Cary,
312 S.C., Hutchins, D.A., 2005. Evaluating vertical migration behavior of harmful

313 raphidophytes in the delaware inland bays utilizing quantitative real-time PCR.
314 Aquat. Microb. Ecol. 40, 121–132.
315 14. Hennige, S.J., Coyne, K.J., Macintyre, H., Liefer, J., Warner, M.E., 2013. The
316 photobiology of *Heterosigma akashiwo*. Photoacclimation, diurnal periodicity,
317 and its ability to rapidly exploit exposure to high light. J. Phycol. 49, 349–360.
318 15. Hu, Q., Sommerfeld, M., Jarvis, E., Ghirardi, M., Posewitz, M., Seibert, M., Darzins,
319 A., 2008. Microalgal triacylglycerols as feedstocks for biofuel production:
320 Perspectives and advances. Plant J. 54, 621–639.
321 16. Hutchins, D.A., Hare, C. E., Weaver, R. S., Zhang, Y., Firme, G. F., DiTullio, Alm,
322 M.B., Riseman, S.F., Maucher, J.M., Geesey, M.R., Trick, C.G., Smith, G.J., Rue,
323 E.L., Conn, R.J., Bruland, K.W., 2002. Phytoplankton iron limitation in the
324 Humboldt current and Peru upwelling. Limnol. Oceanogr. 47, 997–1101.
325 17. Lei, A., Chen, H., Shen, G., Hu, Z., Chen, L., Wang, J., 2012. Expression of fatty acid
326 synthesis genes and fatty acid accumulation in *Haematococcus pluvialis* under
327 different stressors. Biotechnol. Biofuels 5, 1–11.
328 18. Li, Y., Han, D., Hu, G., Sommerfeld, M., Hu, Q., 2010. Inhibition of starch synthesis
329 results in overproduction of lipids in *Chlamydomonas reinhardtii*. Biotechnol.
330 Bioeng. 107, 258–268.
331 19. Molina Grima, E., Belarbi, E.-H., Acién Fernández, F.G., Robles Medina, A., Chisti,
332 Y., 2003. Recovery of microalgal biomass and metabolites: Process options and
333 economics. Biotechnol. Adv. 20, 491–515.

334 20. Nagarajan, S., Chou, S.K., Cao, S., Wu, C., Zhou, Z., 2013. An updated
335 comprehensive techno-economic analysis of algae biodiesel. Bioresour. Technol.
336 145, 150–156.
337 21. Rawat, I., Ranjith, K., R., Mutanda, T., Bux, F., 2013. Biodiesel from microalgae: A
338 critical evaluation from laboratory to large scale production. Appl. Energy 103,
339 444–467.
340 22. Richmond, A., Hu, Q. 2013 Handbook of microalgal culture: Applied phycology and
341 biotechnology, Second edition. Wiley-Blackwell: New York.
342 23. Solovchenko, A., Khozin-Goldberg, I., 2013. High-CO_2 tolerance in microalgae:
343 Possible mechanisms and implications for biotechnology and bioremediation.
344 Biotechnol. Lett. 35, 1745–1752.
345 24. Stewart, J.J., Bianco, C.M., Miller, K.R., Coyne, K.J., 2015. The marine microalga,
346 *Heterosigma akashiwo*, converts industrial waste gases into valuable biomass.
347 Front. Energy Res. 3, doi:10.3389/fenrg.2015.00012.
348 25. Stewart, J.J., Coyne, K.J., 2011. Analysis of raphidophyte assimilatory nitrate
349 reductase reveals unique domain architecture incorporating a 2/2 hemoglobin.
350 Plant. Mol. Biol. 77, 565–575.
351 26. Subramanian, S., Barry, A.N., Pieris, S., Sayre, R.T., 2013. Comparative energetics
352 and kinetics of autotrophic lipid and starch metabolism in chlorophytic
353 microalgae: Implications for biomass and biofuel production. Biotechnol.
354 Biofuels 6, 150.

355 27. Takahashi, H., Clowez, S., Wollman, F.A., Vallon, O., Rappaport, F., 2013. Cyclic
356 electron flow is redox-controlled but independent of state transition. Nat.
357 Commun. 4, 1954.
358 28. Tobin, E.D., Grunbaum, D., Patterson, J., Cattolico, R.A., 2013. Behavioral and
359 physiological changes during benthic-pelagic transition in the harmful alga,
360 *Heterosigma akashiwo*: Potential for rapid bloom formation. PLoS One 8,
361 e76663.
362 29. Warner, M.E., Madden, M.L., 2007. The impact of shifts to elevated irradiance on the
363 growth and photochemical activity of the harmful algae *Chattonella subsalsa* and
364 *Prorocentrum minimum* from Delaware. Harmful Algae 6, 332–342.
365 30. Zhang, Y., Fu, F.-X., Whereat, E., Coyne, K.J., Hutchins, D.A., 2006. Bottom-up
366 controls on a mixed-species hab assemblage: A comparison of sympatric
367 *Chattonella subsalsa* and *Heterosigma akashiwo* (Raphidophyceae) isolates from
368 the Delaware inland bays, USA. Harmful Algae 5, 310–320.

Figure Captions

Fig. 1. Electron transport rates for cultures of *H. akashiwo* previously acclimated to 160, 560, or 1200 µmol quanta m^{-2} s^{-1} after dark acclimation and a subsequent 5 min exposure to 150, 500 or 1200 µmol quanta m^{-2} s^{-1}.

Fig. 2. Carbohydrate, lipid, protein, and chl *a* contents of *H. akashiwo* acclimated to 160, 560, or 1200 µmol quanta m^{-2} s^{-1}.

Fig. 3. Fatty acid profiles of *H. akashiwo* acclimated to 160, 560, or 1200 µmol quanta m^{-2} s^{-1}.

Tables and Figures

Table 1
Growth rates, biomass, and cellular carbon and nitrogen contents in *H. akashiwo* acclimated to 160, 560, or 1200 µmol quanta m^{-2} s^{-1}.

	160	**560**	**1200**
Growth Rate (µ)	0.20 ± 0.04	0.22 ± 0.04	0.18 ± 0.02
Dry Weight (g/L)	0.27 ± 0.12	0.20 ± 0.11	0.26 ± 0.08
Carbon (pg/cell)	819 ± 40 (a)	500 ± 60 (b)	952 ± 270 (a)
Nitrogen (pg/cell)	174 ± 9 (a)	98 ± 18 (b)	176 ± 55 (a)
C/N (mol/mol)	5.48 ± 0.06 (a)	5.96 ± 0.6 (ab)	6.33 ± 0.2 (b)

*Values within rows followed by different letters are significantly different ($P < 0.05$, Tukey's HSD test)

Table 2
Fatty acid saturation type as a percentage of total fatty acid methyl esters in *H. akashiwo* acclimated to 160, 560, or 1200 µmol quanta m^{-2} s^{-1}.

	160	**560**	**1200**
Saturated	41 ± 5	46 ± 6	47 ± 1
Monounsaturated	15 ± 3 (a)	17 ± 1 (ab)	21 ± 3 (b)
Polyunsaturated	44 ± 5 (a)	37 ± 7 (ab)	32 ± 4 (b)

*Values within rows followed by different letters are significantly different ($P < 0.05$, Tukey's HSD test)

Table 3
Calculated parameters for potential biodiesel quality of FAMEs derived from *H. akashiwo* acclimated to 160, 560, or 1200 µmol quanta m^{-2} s^{-1}.

	160	**560**	**1200**
Iodine Number	172 ± 18	148 ± 24	131 ± 11
Saponification Number	204 ± 2 (a)	207 ± 3 (ab)	210 ± 1 (b)
Cetane Number	34 ± 4	39 ± 5	42 ± 2
Cetane Number without 20:5n3*	48 ± 2	52 ± 3	53 ± 2

*Assuming 70% recovery efficiency of 20:5n3
**Values within rows followed by different letters are significantly different ($P < 0.05$, Tukey's HSD test)

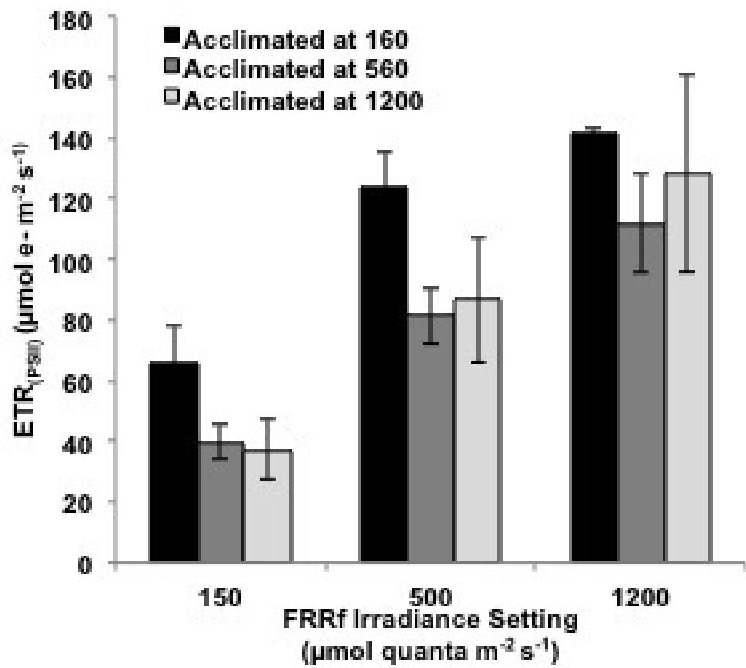

Acclimated at 160
Acclimated at 560
Acclimated at 1200
ETR(PSII) (µmol e- m-2 s-1)
180
160
140
120
100
80
60
40
20
0
150
500
1200
FRRf Irradiance Setting
(µmol quanta m-2 s-1)

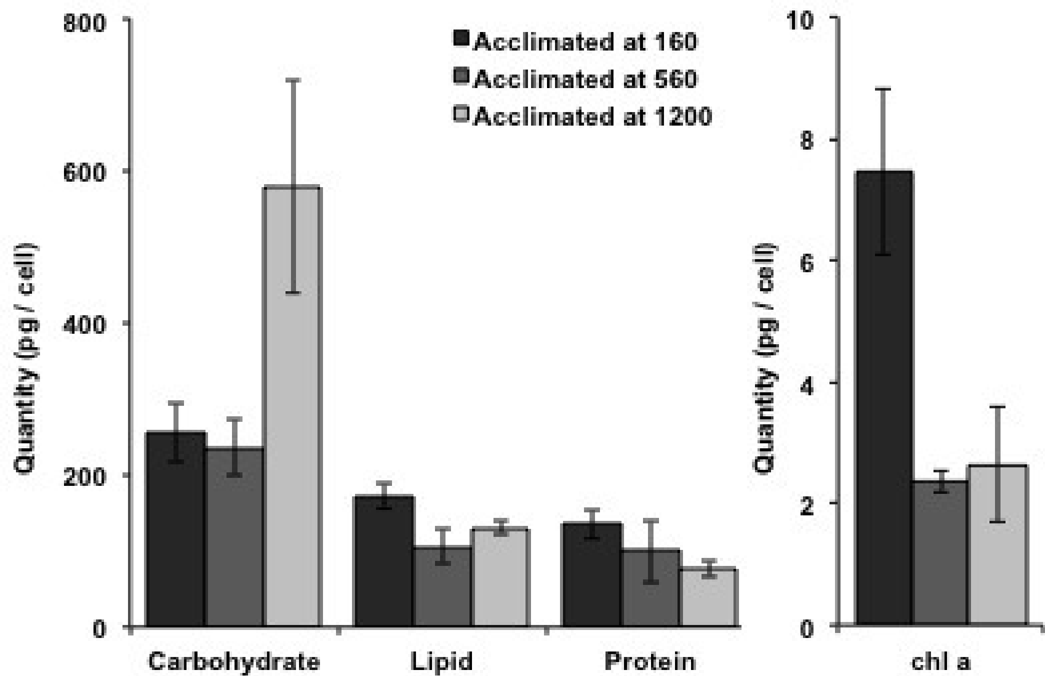

Acclimated at 160
Acclimated at 560
Acclimated at 1200
Quantity (pg / cell)
800
600
400
200
0
Carbohydrate
Lipid
Protein
Quantity (pg / cell)
10
8
6
4
2
0
chl a

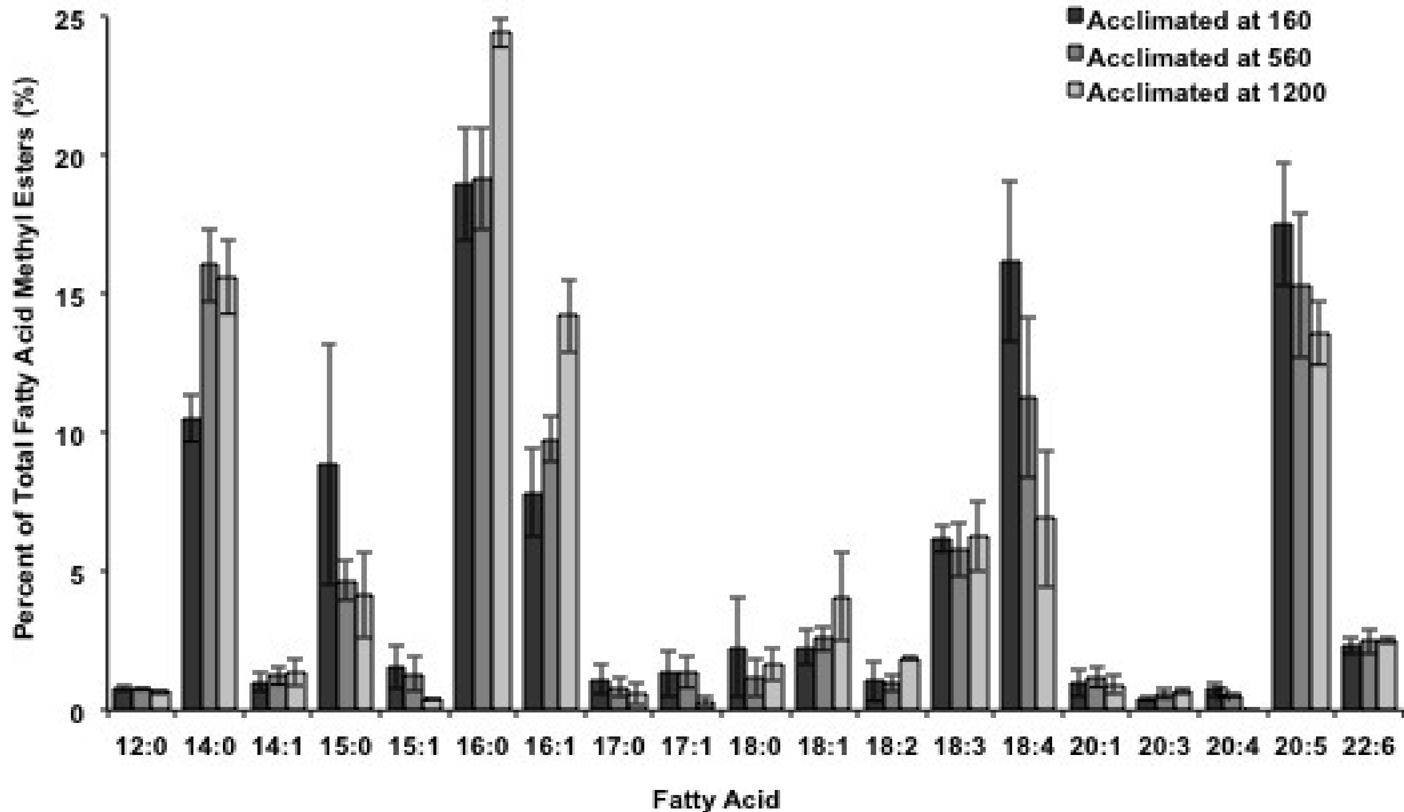

Acclimated at 160
Acclimated at 560
Acclimated at 1200
Percent of Total Fatty Acid Methyl Esters (%)
25
20
15
10
5
0
12:0
14:0
14:1
15:0
15:1
16:0
16:1
17:0
17:1
18:0
18:1
18:2
18:3
18:4
20:1
20:3
20:4
20:5
22:6
Fatty Acid